ISBN: 978-3-95450-217-2 doi:10.18429/JACoW-ERL2019-TUCOXBS01

BEAM HALO IN ENERGY RECOVERY LINACS

O. A. Tanaka†, High Energy Accelerator Research Organization (KEK), Tsukuba, Japan

Abstract

The beam halo mitigation is a very important challenge for reliable and safe operation of a high energy machine. Since Energy Recovery Linacs (ERLs) are known to produce high energy electron beams of high virtual power and high density, the beam halo and related beam losses should be properly mitigated to avoid a direct damage of the equipment, an unacceptable increase in the vacuum pressure, a radiation activation of the accelerator components etc. To keep the operation stable, one needs to address all possible beam halo formation mechanisms, including those unique to each machine that can generate beam halo. Present report is dedicated to the beam halo related activities at the Compact ERL at KEK, and our operational experience with respect to the beam halo.

INTRODUCTION

Beam halo studies and halo mitigation schemes are of the great importance at each stage of accelerator R&D. For those machines that are at their design stage, beam halo studies are limited simply by the absence of the real equipment to perform some tests. Nevertheless, several halo formation mechanisms and processes impacting into the halo could be modeled and estimated prior the machine construction. Here are some of them:

- A space charge effect causes emittance blow-up and bunch lengthening that finally could lead to the formation of the beam halo and consequent beam losses. Examples of space charge effect studies for ERL machines could be found in [1] – [4].
- Effects of the CSR (Coherent Synchrotron Radiation). CSR related issues are in trend nowadays, and addressed in numerous studies (see, for example, [4] – [5]).
- Dark current from the electron gun and longitudinal bunch tails originated at the photocathode [6] – [7].

Other mechanisms could be studied only after the machine construction. One of the examples of the processes enhancing the halo that could not be investigated beforehand is a dark current from RF cavities. Recent results could be found in [8]. Another example is those halo formation mechanisms that are unique for each machine. Thus at the Compact ERL (cERL) at KEK such a unique process was detected and explained for the essential vertical beam halo observed in the end of the injector section and at several locations of the recirculation loop [9]. However, this study was done for the low bunch charge operation (1 pC/bunch, [10]), while the next step operational goal was to achieve a high bunch charge operation (60 pC/bunch, [11]).

Recent industrialization of the cERL beam line [12] imposed new requirements to the beam operation. During last run in June 2019, we optimized injector to the energy 4 MeV [13]. Design parameters dedicated to this run and achieved parameters are listed in the Table 1. Next operational step is to develop the method of beam tuning to control space charge effect. Thus, to be able to produce mid-infrared Free Electron Laser (IR-FEL) light in May 2020, we need to tune the machine for high charge CW operation, while the normalized rms emittance should be kept less than 3π mm mrad, bunch length should be of order of 4 ps, and the energy spread should be minimized to less than 0.062%. These considerations motivated several halo related activities at cERL.

IR-FEL upgrade requires a high bunch charge CW operation. Accordingly, the energy spread should be minimized to improve the FEL-light quality. The halo influence should be studied in this respect. Then, bunch length and beam emittance should be controlled, and we need to exclude the beam halo impact (or reduce as much as possible). Also a reasonable collimation is required to protect the beam line components from its unnecessary activation and to lower the overall beam losses. Collimators should be tested and approved towards the CW operation. Present report is dedicated to these activities and our operational experience with respect to the beam halo.

Table 1: Typical Parameters of CERL Run in June, 2019

Parameter	Design	In operation
Beam energy [MeV]:		
Injector	4	4.05
Recirculation loop	17.6	17.5
Bunch charge [pC]	60	60
Repetition rate [GHz]	1.3	1.3
Bunch length (rms) [ps]	4	4.5
Energy spread [%]	<0.06	0.12
Normalized emittance (rms) in injector [μm·rad]:		
Horizontal	< 3	2.89±0.09
Vertical	< 3	1.99±0.20

HALO TRACKING THROUGH THE INJECTOR

After the injector optics was updated for the energy of 4 MeV, a high bunch charge (60 pC/bunch) beam with a longitudinal bunch tail was tracked through it to compare with observed profiles. To introduce the longitudinal bunch tail into simulations, the initial longitudinal distribution of the bunch was generated in accordance with the curve shown in Figure 1. The core of the bunch is 50 ps FWHM flat-top Gaussian. The backward tail includes 20% of the core intensity. A small (1.5% of the core) forward tail was also added similarly to how it was done in previous beam halo studies [9]. The cutoff of the longitudinal distribution was set to 100 ps. The initial trans-

† olga@post.kek.jp.

ISBN: 978-3-95450-217-2 doi:10.18429/JACoW-ERL2019-TUCOXBS01

verse distribution is assumed to be uniform of 2 mm diameter. Other input parameters for simulations are listed in Table 2. Then, the bunch distribution was tracked with General Particle Tracer code [14] through the injector lattice. The tracking output is compared with measured profiles at Figure 2. We have got a good agreement. One can observe that for a 60 pC bunch the effect of the longitudinal halo is diminished by the beam blow-up due to the space charge effect. Some signs of the horizontal halo could be found at SM#8 location due to nonzero dispersion. Another interesting observation is that tracking without longitudinal tail (only 50 ps rms flat-top Gaussian core) yields exactly same profiles, except at SM#1-2, 8. In that case a central spots disappear. One can conclude that observed central spots are due to the longitudinal bunch tail that is produced at GaAs photocathode.

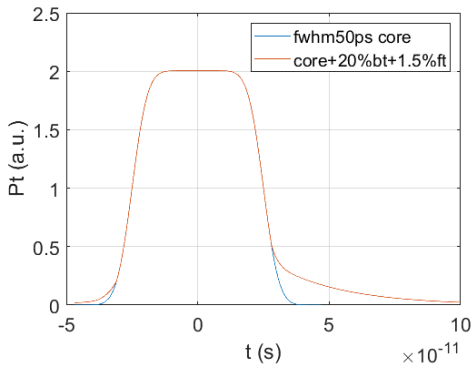

Figure 1: Initial longitudinal distribution at the cathode.

Table 2: Initial Parameters for Injector Tracking

Parameter	Value
Number of particles	25000
Beam energy	4 – 17.5 MeV
Total charge	60 pC / bunch
RF frequency	1.3 GHz
Longitudinal distribution:	
Core	FWHM 50 ps flat-top Gaussian
Tail	Back & forward tails of 100 ps length
Transverse distribution	Uniform φ= 2 mm

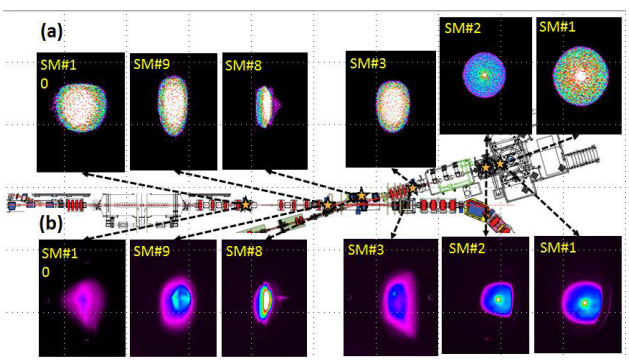

Figure 2: Beam profiles at all injector screen monitor locations: a). Simulated profiles; b). Measured profiles.

COLLIMATOR WAKE STUDY

When the high intensity particle beam passes through locations with narrow apertures, such a collimator's rods, it leads to the creation of the unwanted wake fields. The transverse wake field may affect the beam emittance and the longitudinal wake field can cause the energy loss and the energy spread. The cERL has five collimators (one in the injector section, one in the merger section and three in the recirculation loop, see Fig. 3) to remove the beam halo and to localize the beam loss. An operation at 10 mA average beam current and 1.3 GHz repetition rate is planned in the near future, thus an impact to the collimators together with beam loss reduction issues will become crucial.

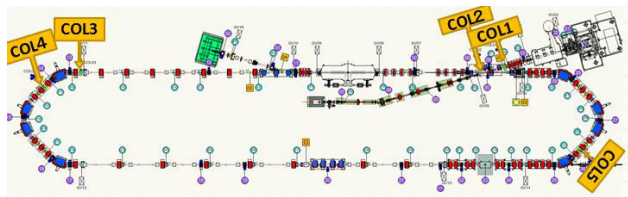

Figure 3: The layout of cERL with collimator's locations.

All cERL collimators consist of four cylindrical rods of 7 mm radius made of copper. They could be independently inserted from the top, bottom, left and right sides of the beam chamber. Collimators COL1 – 3 were designed for the straight sections, therefore they have a round chamber 50 mm radius made of stainless still. Its schematic is given at Fig. 4. Note that the energy at collimators COL 1 – 2 is 4 MeV, while the energy at rest of them is 17.6 MeV. Collimators COL4 – 5 are dedicated to the arc section, thus their chambers are elliptical 70 x 40 mm diameter (Fig. 4).

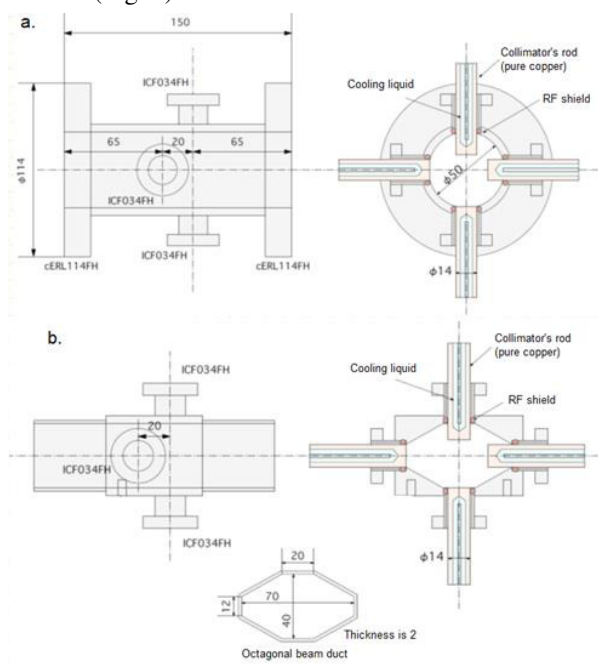

Figure 4: A schematic of the collimators: a). Collimators COL 1 – 3 for the straight sections; b). Collimators COL 4 – 5 for the arc sections.

ISBN: 978-3-95450-217-2 doi:10.18429/JACoW-ERL2019-TUCOXBS01

Transverse Wake and Emittance Growth

Let us consider first transverse wake fields created by the vertical rods of the collimator. The summary of CST Particle Studio [15] simulation results together with analytical calculations for 2 ps bunch length is demonstrated at Fig. 5. We have estimated the emittance blow-up for the 60 pC electron bunch at cERL using analytical expression [16]:

$$\frac{\Delta\varepsilon_y}{\varepsilon_{y0}} = \sqrt{1+\frac{\beta_y\sigma_\omega^2}{\varepsilon_{y0}}} - 1, \quad (1)$$

where the value $\Delta\varepsilon_y$ is the transverse emittance growth with respect to the initial emittance ε_{y0}. The rms of the centroid kicks caused by the longitudinally varying field σ_ω could be found as follows [17]:

$$\sigma_\omega = \frac{Q}{E/e} k_\perp^{rms} y_0. \quad (2)$$

In Eq. (2) the value E is the beam energy at the location of collimator. The value $Q = 60\,pC$ is the bunch charge. The value y_0 is the beam centroid offset, and lastly, the value $k_\perp^{rms}$ is the rms kick factor, estimated for the bunch head-tail difference in the kick. For Gaussian bunch $k_\perp^{rms} = k_\perp/\sqrt{3}$.

Expected values of the emittance blow-up due to the collimator half gap 1.5 mm are summarized in Table 3.

Since for 60pC per bunch and burst mode of the operation the emittance growth effect is expected to be small, let us treat longitudinal wake.

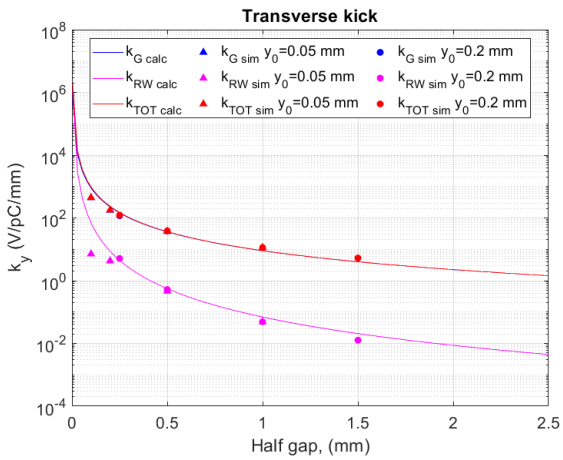

Figure 5: A summary of the transverse wake kick factors of the collimators.

Table 3: Expected Values of the Emittance Blow-Up for the Collimator Half Gap 1.5 mm

Collimator	ε_{y0} [μm×rad]	β_y [m]	$\Delta\varepsilon_y/\varepsilon_{y0}$ [%]
COL1 E=4 MeV	1.15	27.47	1.05
COL2 E=4 MeV	1.25	19.23	0.84
COL3 E=17.6 MeV	0.954	34.76	3.82
COL4 E=17.6 MeV	0.954	6.99	1.61
COL5 E=17.6 MeV	0.954	6.99	1.61

Longitudinal Wake and Energy Spread

Now, let us consider a problem of longitudinal wake fields excited by collimators. The values of the wake-loss factor were evaluated numerically through the CST simulation for half-gap values in the range from 0.1 to 1.5 mm. The dependence of the energy spread on the collimator's half gap for the designed (2 ps) and current (4.5 ps) bunch length is demonstrated at Fig. 6. For the analytical description, the following equation was considered [18]:

$$k_\parallel = \frac{Z_0 c}{2\pi^{3/2}\sigma_z}\ln\left(\frac{b}{a}\right). \quad (3)$$

In Eq. (3) the value $Z_0=120\pi$ is the impedance of the free space, c = $3\cdot10^8$ m/s is the speed of light, σ_z is the bunch length, b = 25 mm is the vacuum duct's half aperture, and a is the collimator's half gap.

The energy loss per whole bunch at one collimator for the 60 pC per bunch burst mode at the bunch length 2 ps, and for the collimator half gap 1.5 mm is:

$$\Delta E = k_\parallel Q^2 = 46.86V/pC \times (60\,pC)^2 = 168.7nJ. \quad (4)$$

The voltage received by the electrons is $\Delta V = k_\parallel \times Q = 2812$ V. The energy change in one electron is reduced by $e\Delta V = 2812$ eV. If E=17.6 MeV, the change of energy peak is $e\Delta V/E = 2816$ eV/17.6 MeV=0.016%. For Gaussian bunch the energy spread due to one collimator is $\sigma E = 0.4\times k_\parallel \times Q = 1124$V. With respect to the beam energy E=17.6 MeV the wake-induced energy spread reads $\sigma E/E = 1124$ eV/17.6 MeV=0.0063%. Unfortunately estimated values are beyond the limits of the resolution of our monitors, and it is unlikely we could detect them.

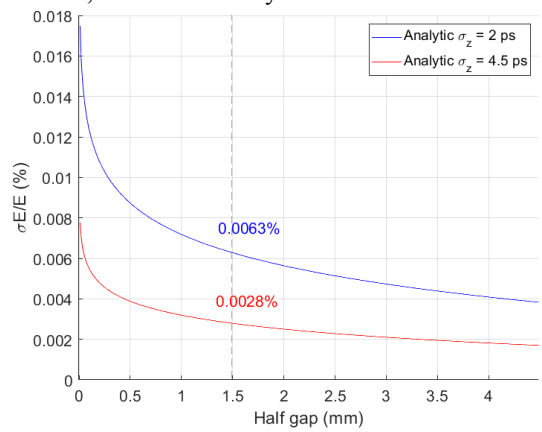

Figure 6: A wake-induced energy spread for different values of the collimator half gap and bunch lengths 2 ps (blue line) and 4.5 ps (red line).

BEAM-BASED MEASUREMENTS

Energy Spread Measurement

For the measurement of the energy spread caused by the collimator's longitudinal wake, we used COL3 located before first arc entrance, SM#13 located between COL3 and the entrance of the are section and SM#15 located just in the middle of the arc (see Fig. 3). SM#13 needed to monitor the beam spot, which was successively cut by collimator's rods. The measurement itself was done by SM#15. To do so, first, we have restored the

ISBN: 978-3-95450-217-2 doi:10.18429/JACoW-ERL2019-TUCOXBS01

history of the quadrupole magnets to have the best beam spot at the COL3 location. Then we have degaussed all quadrupoles of the first arc between SM#13 and SM#15 to make the dispersion maximized. We have measured the dispersion to be 2.41 m. The default energy spread was $\sigma E/E_{default}=\sigma_x/\eta=0.117\%$. It is a ratio of the rms beam size to the dispersion. However, in the following we care only the change of the energy spread, not its default value.

Next step was to insert the collimator COL3. We used two horizontal rods, because the beam spot at the collimator location is known for its vertical beam halo. Therefore, we have avoided an influence of the halo on our energy spread measurement. We have performed the measurement for the half gap values 2 mm, 1.5 mm, 2 mm, 2.5 mm, 4 mm, COL out correspondingly. Related rms beam sizes and beam profile peak positions were recorded at SM#15. The raw data of the beam profile was fitted by Gaussian fitting routine and weight analysis. An example of the measurement data processing could be found at Fig. 7. Here the upper image is a SM#15 beam spot, the blue curve at the bottom plot is the raw data, the red line is its Gaussian fitting, and the magenta mark denotes the peak position with respect to the data weight.

Weight analysis [19] gives the following expression for the profile peak position:

$$x_c = \frac{1}{N}\sum_{i=1}^{659} x_i N_i, \quad where \quad N = \sum_{i=1}^{659} N_i. \tag{5}$$

Here N is the number of data points, and x_i is the value of the ith data point. The rms beam size is given by:

$$\sigma_x = \sqrt{\frac{1}{N}\sum_{i=1}^{659} N_i \left(x_i - x_c\right)^2}. \tag{6}$$

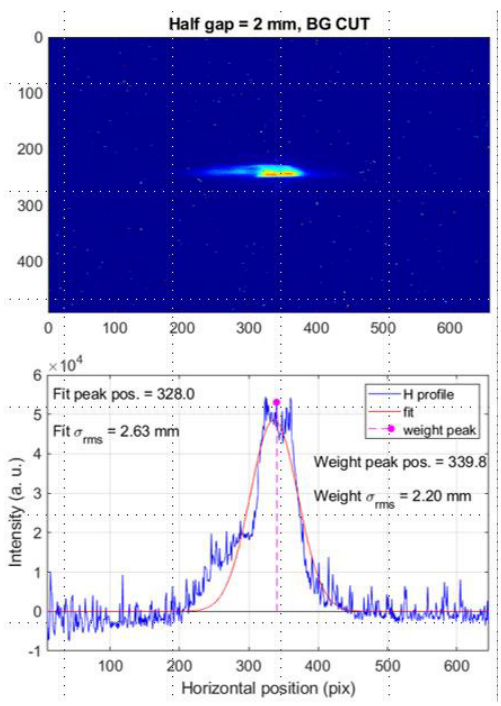

Figure 7: Energy spread measurement data at SM#15: beam spot (top), raw data and its fitting (bottom).

Results of the processing of all six measurements are demonstrated at Fig. 8. The rms beam size is not changed significantly within the error bar except in the case of the 1.5 mm half gap. It was a prediction by simulation and calculation. The beam size drop at the half gap 1.5 mm indicates that the beam core was damaged by the collimator's rod.

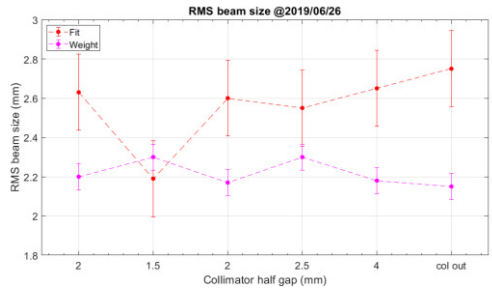

Figure 8: A horizontal beam size at SM#15 with respect to the horizontal collimation: fitting result (red), weight analysis result (magenta).

Beam Halo Influence

The location of the collimator COL3 (before the arc entrance, Fig. 3) is known for the considerable vertical beam halo [7]. The correspondent beam spot at SM#13 is shown at Fig. 9. Thus, by inserting vertical rods of the collimator COL3, one can study the beam halo influence on the energy spread and consequently manage the beam quality by removing the halo by the collimator.

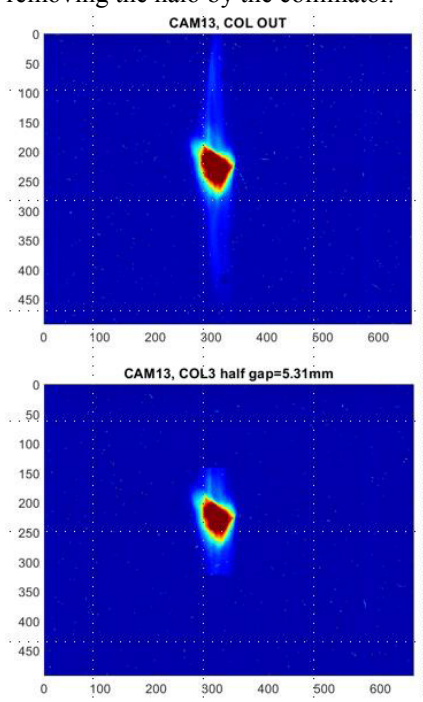

Figure 9: A beam spot at CAM13: without (top), and with (bottom) the collimation.

To study this effect, we performed the same measurements as was described in the previous section. Although the vertical collimation was allowed. A series of four measurements was done. The collimator's half gap was set to 5.31 mm, 5.75 mm, 6.25 mm, and COL3 out corre-

ISBN: 978-3-95450-217-2 doi:10.18429/JACoW-ERL2019-TUCOXBS01

spondingly. Then the proper data processing gave results, presented at Fig. 10. One can see the horizontal beam size is slightly decreased with the cutting away the vertical beam halo. The energy spread also became smaller.

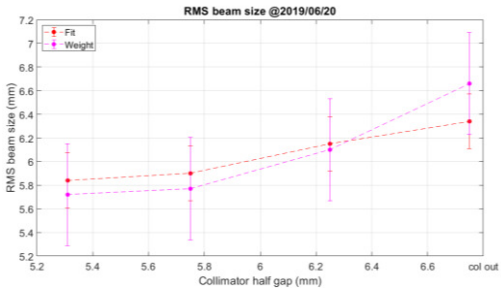

Figure 10: Horizontal beam size at SM#15 with respect to the vertical collimation: fitting result (red), weight analysis result (magenta).

CONCLUSION AND OUTLOOK

Halo related discussion does not seem to be a trend nowadays. Nevertheless, the problem of the beam halo addresses to a numerous issues at all stages of accelerator machine R&D.

Experimentally we have found, that for current beam parameters (bunch charge is 60 pC (burst mode), bunch length is 4.5 ps, energy spread is ~0.12%, beam energy is 17.5 MeV (injector energy is 4.05 MeV)) even if one put the half gap of the collimator up to 2 mm, the emittance and energy spread are not affected so much. Thus we approved the beam collimation at cERL.

The additional energy spread due to collimator's wake at cERL is found to be 0.0028 % at 17.5 MeV, which is negligibly small.

Considering future cERL upgrade to the IR-FEL, a possibility of consequent degradation of the FEL performance should be taken into account. Correspondent power loss was obtained as 13.7 W (81.25 MHz, 5 mA, 2 ps).

At cERL like at any other ERL facility, we have to consider the halo seriously for the beam current increase (up to 10 mA at cERL), since without due care the beam loss problem would be unavoidable.

ACKNOWLEDGEMENTS

This research is carried out with the support of NEDO project "Development of next generation laser technology with high brightness and high efficiency".

REFERENCES

[1] https://arxiv.org/pdf/1706.04245.pdf

[2] https://arxiv.org/pdf/1705.08783.pdf

[3] B. Kuske, "Adjusting bERLinPro optics to commissioning needs", presented at the 60th ICFA Advanced Beam Dynamics Workshop on Energy Recovery Linacs (ERL19), Berlin, Germany, September 2019, this conference.

[4] M. Abo-Bakr, "Beam dynamics and optics challenges of bERLinPro", presented at the 59th ICFA Advanced Beam Dynamics Workshop on Energy Recovery Linacs (ERL17), Geneva, Switzerland, Jun. 2017, paper WEIBCC003, unpublished.

[5] W. Lou *et al.*, "Coherent synchrotron radiation simulation for CBETA", in *Proc. IPAC'19*, Melbourne, Australia, May 2019, pp. 406-409. doi:10.18429/JACoW-IPAC2019-MOPGW124

[6] M. McAteer, "Dark current and halo tracking in ERLs", presented at the 59th ICFA Advanced Beam Dynamics Workshop on Energy Recovery Linacs (ERL17), Geneva, Switzerland, Jun. 2017, paper THIACC002, unpublished.

[7] O. Tanaka, "Beam halo study at the KEK compact ERL", presented at the 59th ICFA Advanced Beam Dynamics Workshop on Energy Recovery Linacs (ERL17), Geneva, Switzerland, Jun. 2017, paper THICCC001, unpublished.

[8] A. Neumann *et al.*, "The bERLinPro SRF photo injector system – from first RF commissioning to first beam", in *Proc. IPAC'18*, Vancouver, BC, Canada, Apr.-May 2018, pp. 1660-1663. doi:10.18429/JACoW-IPAC2018-TUPML053

[9] O. Tanaka *et al.*, "New halo formation mechanism at the KEK compact energy recovery linac", *Phys. Rev. Accel. Beams*, vol. 21, p. 024202, Feb. 2018. doi:10.1103/PhysRevAccelBeams.21.024202

[10] M. Akemoto *et al.*, "Construction and commissioning of the compact energy-recovery linac at KEK", *Nucl. Instrum. Methods*, vol. 877, pp. 197-218, 2018. doi: 10.1016/j.nima.2017.08.051

[11]T. Miyajima, "Higher bunch charge operation in Compact ERL at KEK", presented at the 59th ICFA Advanced Beam Dynamics Workshop on Energy Recovery Linacs (ERL17), Geneva, Switzerland, Jun. 2017, paper THIACC001, unpublished.

[12] H. Sakai, "Industrial applications of cERL", presented at the 60th ICFA Advanced Beam Dynamics Workshop on Energy Recovery Linacs (ERL19), Berlin, Germany, September 2019, this conference.

[13] T. Miyajima, "Injector development at KEK", presented at the 60th ICFA Advanced Beam Dynamics Workshop on Energy Recovery Linacs (ERL19), Berlin, Germany, September 2019, this conference.

[14] S. B. van der Geer and M. J. de Loos, *The General Particle Tracer code: Design, Implementation and Application*, Technische Universiteit Eindhoven, Eindhoven, 2001.

[15] CST-Computer Simulation Technology, CST PARTICLE STUDIO. http://www.cst.com/Content/Products/PS/Overview.aspx

[16] M. Dohlus, T. Limberg, "Impact of Optics on CSR-Related Emittance Growth in Bunch Compressor Chicanes", in Proc. of 21st Particle Accelerator Conference (PAC05), Knoxville, USA, May. 2005.

[17] S. Di Mitri, "Geometric efficiency of a two-stage fully absorbing collimation system in single-pass linacs", *Phys. Rev. ST Accel. Beams,* vol. 13, p. 052801, May 2010. doi: 10.1103/PhysRevSTAB.13.052801

[18] S. Heifets and S. Kheifets, "Coupling impedance in modern accelerators", *Rev. Mod. Phys.* vol. 63, p. 631, Jul. 1991. doi:10.1103/RevModPhys.63.631

[19] P. R. Bevington and D. K. Robinson, *Data Reduction and Error Analysis for the Physical Sciences*, McGraw-Hill, 1992.